Hydrogen bonding to carbonyl hydride complex Cp*Mo(PMe3)2(CO)H and its role in proton transfer

Pavel Dub, Oleg A Filippov, Natalia V Belkova, Jean-Claude Daran, Lina M Epstein, Rinaldo Poli, Elena S Shubina

Hydrogen bonding to carbonyl hydride complex $Cp^*Mo(PMe_3)_2(CO)H$ and its role in proton transfer

Pavel A. Dub,[a,b] Oleg A. Filippov,[a] Natalia V. Belkova,*[a] Jean-Claude Daran,[b] Lina M. Epstein,[a] Rinaldo Poli*[b,c] and Elena S. Shubina*[a]

Received (in XXX, XXX) Xth XXXXXXXXX 200X, Accepted Xth XXXXXXXXX 200X
First published on the web Xth XXXXXXXXX 200X
DOI: 10.1039/b000000x

The interaction of the carbonyl hydride complex $Cp^*Mo(PMe_3)_2(CO)H$ with Brønsted (fluorinated alcohols, $(CF_3)_nCH_{3-n}OH$ (n = 1-3), and CF_3COOH) and Lewis ($Hg(C_6F_5)_2$, $BF_3{\cdot}OEt_2$) acids was studied by variable temperature IR and NMR (^1H, ^{31}P, ^{13}C) spectroscopies in combination with DFT/B3LYP calculations. Among the two functionalities potentially capable for the interaction - carbonyl and hydride ligands – the first one was found to be the preferential binding site for weak acids, yielding CO···HOR or CO···Hg complexes as well as the CO···$(HOR)_2$ adducts. For stronger proton donors ($(CF_3)_3COH$, CF_3COOH) hydrogen-bonding to the hydride ligand can be revealed as an intermediate of the proton transfer reaction. Whereas proton transfer to the CO ligand is not feasible, protonation of the hydride ligand yields an (η^2-H_2) complex. Above 230 K dihydrogen evolution is observed leading to decomposition. Among the decomposition products compound $[Cp^*Mo(PMe_3)_3(CO)]^+[(CF_3)_3CO{\cdot}2HOC(CF_3)_3]^-$ resulting from a phosphine transfer reaction was characterized by X-ray diffraction. Reaction with $BF_3{\cdot}OEt_2$ was found to produce $[Cp^*Mo(PMe_3)_2(CO)BF_4]$ via initial attack of the hydride ligand.

Introduction

Being among the earliest discovered organometallic complexes, metal carbonyls continue to play one of the central roles in organometallic chemistry.[1,2] Addition of the hydride function to a transition metal carbonyl complex results in the formation and coexistence of three potentially basic centers inside the carbonyl hydride complex: the metal atom, the hydride ligand and the CO-oxygen atom. With the exception of bridging carbonyl ligands,[3] protons from strong acids usually add to the metal atom or to the hydride ligand.[4] On the other hand, much bulkier Lewis acids generally add to carbonyl oxygens.[2] Weak proton donors (mostly alcohols) interact with either the hydride ligand or the CO-oxygen.[4,5] Very recently we have reported the results of the protonation of the carbonyl hydride complex $Cp^*Mo(PMe_3)_2(CO)H$ (**1**) by the strong acid HBF_4. At low temperatures proton transfer in THF yields the dihydrogen complex $[Cp^*Mo(PMe_3)_2(CO)(\eta^2\text{-}H_2)]BF_4$ as a sole observable protonation product, however when the same reaction is carried out in CH_2Cl_2 the only product of the reaction is the cationic dihydride complex $[Cp^*Mo(PMe_3)_2(CO)(H)_2]BF_4$.[6] The stability of the $[Cp^*Mo(PMe_3)_2(CO)H_2]BF_4$ ion pair and the classical/non-classical equilibrium appeared to be fine tuned by the series of cation-anion-solvent non-covalent interactions. In order to get further insight into the proton transfer mechanism we performed a more detailed study of the interaction between **1** and series of Brønsted acids (fluorinated alcohols $(CF_3)_nCH_{3-n}OH$ (n = 1-3) and trifluoroacetic acid) , as well as a few selected Lewis acids.

Results

Compound **1** was first described by Lapinte *et al*[7] and obtained in a pure form by Parkin *et al* upon reaction of $Cp^*Mo(PMe_3)_3H$ with CO.[8] It possesses catalytic activity in the decomposition of HCO_2H to CO_2 and H_2 and was found to react with RCOOH (R = H, Me, Et) at room temperature, leading to dihydrogen evolution and $Cp^*Mo(PMe_3)_2(CO)(\eta^1\text{-}O_2CR)$.[8] This result suggests the presence of the (η^2-H_2) complex along the reaction coordinate. The initial attack by fluorinated alcohols was therefore expected to take place at the hydride site yielding a dihydrogen bonded complex as a reaction intermediate.[9,10] Dihydrogen-bonding is known[11] to induce a high field shift of the ^1H NMR hydride resonance and a decrease of its longitudinal relaxation time (T_{1min}), whereas in the IR spectra it causes a low frequency shift of the $\nu_{M\text{-}H}$ band and a high frequency shift of the characteristic bands of all other ligands, such as e.g. ν_{CO}.[11] To our surprise the addition of 2 equiv CF_3CH_2OH (TFE) to the solution of **1** in CD_2Cl_2 at 200K resulted in a low field shift of the hydride resonance ($\Delta\delta$ = 0.19 ppm; $\Delta\delta \equiv \delta(\mathbf{1} + ROH) - \delta(\mathbf{1})$), see Fig. 1. The measured value of T_1 (930 ms at 500 MHz, 200 K) was a bit higher than that of the starting material (860 ms under the same conditions). Further TFE addition (4.5 equiv total) led to a greater shift of the resonance ($\Delta\delta$ = 0.29 ppm) and T_1 = 900 ms. The direction of the signal shift together with nonlinear T_1 dependence suggest that the hydride ligand is not interacting with TFE.

The Cp* and PMe_3 proton resonances of **1** showed practically no change following the addition of excess TFE in this solvent (Table 1). However, the $^{31}P\{^1H\}$ signal is sensitive to the presence of the alcohol, shifting by $\Delta\delta$ = -0.4 (with 2 equiv TFE) to -0.6 ppm (4.5 equiv TFE).

Table 1. Selected NMR (^{1}H, ^{31}P{^{1}H}, ^{13}C{^{1}H}) parameters for complex **1** in different solvents in the presence of proton donors at 200 K.

solv	ROH	[ROH]/[**1**]	δ_H [a]	δ_H(Cp*)	δ_H(PMe$_3$) [b]	δ_P	δ_{CO} [c]
CD_2Cl_2		0	-6.98 (t)	1.89 (s)	1.31 (d)	31.4 (s)	255.0 (t)
	TFE	2.0	-6.79 (t)	1.89 (s)	1.31 (d)	31.0 (s)	
		4.5	-6.69 (t)	1.89 (s)	1.31 (d)	30.8 (s)	257.5 (t)
tol-d_8		0	-6.85 (t)	1.96 (s)	1.34 (d)	31.9 (s)	253.1 (t)
	TFE	3.7	-6.57 (t)	2.02 (s)	1.42 (d)	30.7 (s)	
tol-d_8 [d]		0	-6.88 (t)	1.93 (s)	1.33 (d)	30.3 (s)	253.1 (t)
	TFE	3.7	-6.78 (t)	1.95 (s)	1.35 (d)	29.9 (s)	
	PFTB	2.0	-6.38 (t)	1.82 (s)	1.21 (d)	30.1 (s)	259.2 (t)

[a] An invariant $^2J_{HP}$ of 77 Hz was measured under all conditions; [b] An invariant $^2J_{HP}$ of 8 Hz was measured under all conditions ; [c] An invariant $^2J_{CP}$ = 28 Hz was measured under all conditions; [d] at 298K.

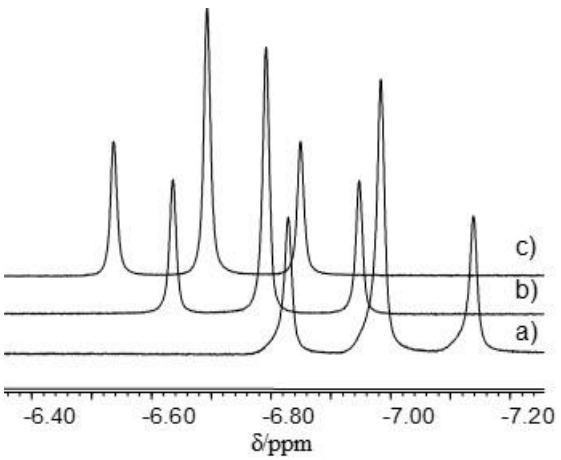

Fig. 1. Hydride region of the ^{1}H NMR (500.3 MHz) spectrum of **1** alone(a), and in the presence of 2 equiv (b) or 4.5 equiv (c) of TFE. T = 200K, CD_2Cl_2, c(**1**) = $5.8\cdot10^{-2}$ M.

Addition of TFE (3.7 equiv) to the solution of **1** in the less polar toluene-d_8 at 200K causes again a low field shift ($\Delta\delta$ = 0.28 ppm) of the hydride resonance and a high-field shift ($\Delta\delta$ = -0.9 ppm) of the ^{31}P{^{1}H} signal. In this solvent the Cp* and PMe$_3$ proton resonances are quite sensitive to the acid addition, each shifting to higher field by $\Delta\delta$ = -0.08 ppm (Table 1).

The dependence of all the chemical shifts on the TFE amount suggests the presence of equilibrium in the system. Indeed, when the temperature of the toluene solution of **1** with 3.7 equiv TFE was raised to 290K, all the resonances $\Delta\delta$ values decreased, in agreement with an equilibrium shift toward starting material upon warming ($\Delta\delta_H$ = 0.10 ppm, $\Delta\delta_{Cp^*H}$ = $\Delta\delta_{PMe3}$ = -0.02 ppm, $\Delta\delta_P$ = -0.4 ppm), see Table 1. The process is completely reversible, the signal shifts restoring their values upon cooling back to 200 K.

Finally, the low temperature (200K) ^{13}C{^{1}H} NMR study in toluene-d_8 revealed that the characteristic triplet of the CO resonance of **1** ($^2J_{C-P}$ = 29 Hz) at δ 253.1 (Fig. 2) shifts downfield by 6.1 ppm in the presence of 2 equiv of $(CF_3)_3COH$ (PFTB). Other signals have $\Delta\delta_{C(C5Me5)}$ = 1.1 ppm, $\Delta\delta_{C(PMe3)}$ = -0.7 ppm, $\Delta\delta_{C(C5Me5)}$ = -0.5 ppm). Like in the case of $\Delta\delta_H$ and $\Delta\delta_P$, the $\Delta\delta_C$ depends on the acid amount, the temperature and the solvent. In more polar CD_2Cl_2, use of TFE at 200K gives $\Delta\delta_{CO}$ = 2.3 ppm (3.3 equiv) and 2.5 ppm (4.5 equiv). Attachment of an acceptor to the oxygen end of the CO ligand is known to shift the ^{13}CO resonance downfield.[2] Together with the IR spectroscopic results (see below), this allows to suggest the formation of a CO···HOR^F hydrogen bond.

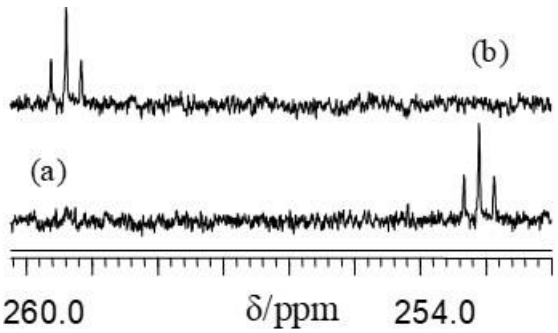

Fig. 2. ^{13}C{^{1}H} NMR (125.8MHz, CO region) spectrum of 1 (a) and 1 in the presence of ca. 2 equiv PFTB (b). toluene-d_8, 200K. c(1) = $1\cdot10^{-1}$ M, 1330 scans.

The IR spectra in the TFE ν_{OH} region in CH_2Cl_2 showed the typical picture of hydrogen bond formation in the presence of **1**. The intensity of the ν_{OH} band of the free alcohol decreased and a new wide band of hydrogen bonded TFE appeared at lower frequency. The addition of ca. 3 equiv TFE to the solution of **1** in hexane at 200K caused a decrease of the ν_{CO}(**1**) band intensity and the appearance of two new bands, ν_{CO}(**1a**) at 1736 and ν_{CO}(**1b**) at 1720 cm^{-1} (Fig. 3). When the temperature was raised to 250K the 1720 cm^{-1} band completely disappeared and only traces of the 1736 cm^{-1} band remained, while the intensity of the band of the starting material increased. Cooling back to 200 K reproduced fully the initially observed picture, demonstrating the reversibility of the process. More acidic proton donors, $(CF_3)_2CHOH$ (HFIP) and PFTB, forming stronger hydrogen bonds, give more intense bands (with lower intensity of the ν_{CO}(**1**)) at even lower frequencies (Fig. 3, Table 2). These changes indicate a progressive shift of the hydrogen bonding equilibrium to the right with an increase of the alcohol proton donating ability.

Table 2. Parameters of the ν_{CO} bands for hydrogen bonded complexes of **1** with alcohols at 200 K.

Solv	ROH	[ROH]/[**1**]	ν_{CO}(**1**)	ν_{CO}(**1a**)	ν_{CO}(**1b**)
hexane		0	1791		
	TFE	10	1791	1738	1720
	HFIP	5	1791	1732	1718
	PFTB	5	1791	1727	1716
toluene		0	1771		
	PFTB	5	1771	1707	1695

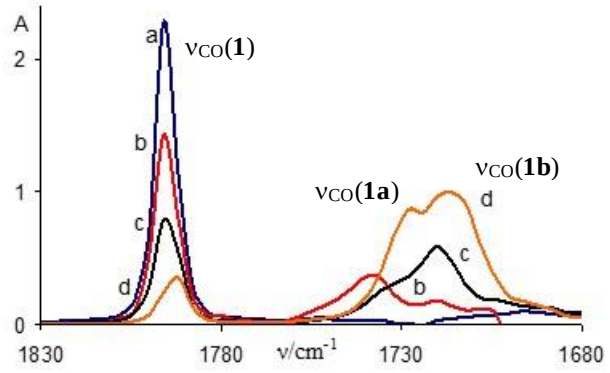

Fig. 3. IR spectra (ν_{CO} region) of Cp*Mo(PMe_3)$_2$(CO)H (1) (0.005 M) (a) and in the presence of ca. 3 equiv. TFE (b), 3 equiv HFIP (c), 3 equiv PFTB (d). T = 200K, hexane, l = 1.2 mm.

The low frequency ν_{CO} shift in the presence of proton donors is evidence for hydrogen bonding with the carbonyl ligand.[12,5] Appearance of a second ν_{CO} band, shifted by -11 to -18 cm^{-1} in respect to ν_{CO}(**1a**), indicates formation of yet another H-bonded complex, which we believe contains CO···HO bond with the alcohol dimer (Scheme 1). Note that binding of the second alcohol molecule at the hydride ligand would shift the ν_{CO} band to higher frequency relative to ν_{CO}(**1a**).[5] The nature of the hydrogen bonded species **1a** and **1b** was further assessed with the help of DFT calculations.

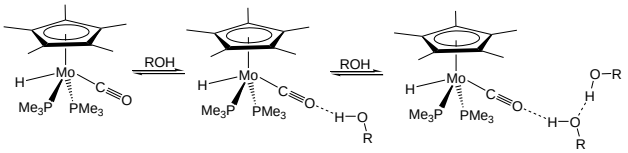

Scheme 1

Geometry optimization and frequency calculations were performed for hydride **1** and for its hydrogen bonded complexes with CH_3OH, CF_3OH and CF_3COOH at DFT/B3LYP level. Coordination of proton donors at the carbonyl and hydride ligand sites was considered as well as possible complexes with two proton donor molecules. The structures obtained are exemplified for the case of CH_3OH in Fig. 4, interaction energies and spectroscopic parameters are gathered in Table 3, and selected geometrical characteristics are given in the ESI† (Table S2). Formation energies (Table 3) obtained for complexes with one HOR molecule show preference for classical CO···HOR bonding over non-classical MoH···HOR interaction for methanol, which becomes less significant for stronger proton donors. BSSE correction reduces formation energies by 14-35% but the ΔE_{BSSE} pattern is similar to that of ΔE's (Table 3).

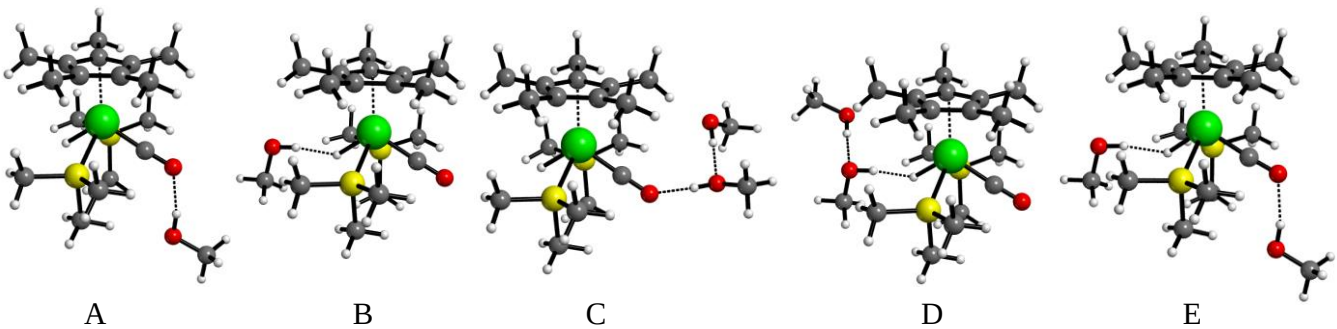

Fig. 4. Optimized geometries of hydrogen bonded complexes between **1** and one and two CH_3OH molecules.

Table 3. Formation energies (relative to the separated reactants, in kJ mol^{-1}) and frequencies (in cm^{-1}) calculated for H-complexes between **1** and proton donors in gas phase.

Proton donor	H-complex notation	H-bond type	ΔE	ΔE_{ZPVE}	ΔE_{BSSE}	ΔH ($\Delta\nu_{OH}$) [a]	ν_{CO} ($\Delta\nu_{CO}$) [b]	$\Delta\nu_{OH}$ [c]
CH_3OH	**A**	CO···HOR	-25	-19	-22	-13	1813 (-50)	-142
	B	H···HOR	-20	-15	-15	-20	1865 (+2)	-261
$2CH_3OH$	**C**	CO···$(HOR)_2$	-58	-46	-49	-16	1799 (-64)	-188
	D	H···$(HOR)_2$	-54	-41	-42	-26	1866 (+3)	-374
	E	CO···HO & H···HO	-45	-35	-36	-12 & -19	1813 (-50)	-138 & -249
CF_3OH	**A**	CO···HOR	-62	-58	-46	-34	1780 (-83)	-582
	B	H···HOR	-61	-56	-39	-45	1872 (+9)	-1048
CF_3COOH	**A**	CO···HOR	-53	-49	-46	-34	1750 (-113) 1808 (-55)[d]	-589
	B	H···HOR	-47	-44	-36	-43	1876 (+13)	-964
$2CF_3COOH$	**C**	CO···$(HOR)_2$	-100	-92	-77	-41	1709 (-154) 1776 (-87)[d]	-875
	D	H···$(HOR)_2$	-90	-85	-67	-49	1879 (+16)	-1348
	E	CO···HO & H···HO	-95	-88	-76	-31 & -42	1768 (-95), 1812 (-51)[d]	-512 & -890

[a] enthalpy values based on calculated $\Delta\nu_{OH}$: ΔH (in kJ mol^{-1}) = $-75\Delta\nu/(\Delta\nu+720)$[13,14]; [b] $\Delta\nu_{CO}$ = ν_{CO}(complex) - ν_{CO}(**1**), ν_{CO}(**1**) = 1863 cm^{-1}; [c] $\Delta\nu_{OH}$ = ν_{OH}(complex) - ν_{OH}(HOR); [d] TFA has the ν_{CO} mode in this range, therefore the ν_{CO} vibrations of **1** and TFA are mixed

In the case of interaction with two proton donor molecules (calculated for CH_3OH and CfigurF$_3$COOH), two adducts with the HOR dimer, CO···$(HOR)_2$ (**C**) and MoH···$(HOR)_2$ (**D**), as well as of complexes with simultaneous hydrogen bonding to carbonyl and hydride ligands, ROH···(OC)MoH···HOR (**E**), were optimized leading to stable energy minima. The formation energy for the latter complex (Table 3) is equal to the sum of two interactions (CO···HOR and MoH···HOR) for methanol, whereas mutual weakening of the two hydrogen bonds (anticooperativity[15]) was found in complex **E** for TFA (by 5 kJ mol^{-1}). A cooperativity effect is observed for the formation of **C** and **D** [ΔE_{coop} = ΔE(**1**·2HOR) - ΔE(**1**·HOR) - ΔE((HOR)$_2$)], -7 and -13 kJ mol^{-1} for **C** and –8 and -9 kJ mol^{-1} for **D** with CH_3OH and CF_3COOH, respectively, showing the decrease of the relative impact of the cooperative effect into total formation energy ($\Delta E_{coop}/\Delta$E(**1**·2HOR)) for stronger proton donor.

As can be seen from the Table 3, hydrogen bonding to the CO ligand leads to a low frequency shift of the ν_{CO} band, whereas H···H bond formation leads to a high frequency ν_{CO} shift. In agreement with our experimental data, $\Delta\nu_{CO}$ increases with the proton donor strength. According to the calculations, the experimentally observed ν_{CO}(**1b**) band could certainly be assigned to species **C**. The ν_{CO}(**1a**) band, on the other hand, could be generated not only by complex **A**, but also by complex **E**. Dihydrogen bonded complexes of **B** or **D** type should appear at frequencies higher than ν_{CO}(**1**).

$$Cp^*MoH(CO)(PMe_3)_2 + H^+ \rightarrow [Cp^*MoH(COH)(PMe_3)_2]^+ \quad (1)$$

$$Cp^*MoH(CO)(PMe_3)_2 + H^+ \rightarrow [Cp^*Mo(\eta^2\text{-}H_2)(CO)(PMe_3)_2]^+ \quad 2)$$

Protonation of the carbonyl ligand (Equation 1) was found less exothermic by $\Delta\Delta$E = 85 kJ mol^{-1} than protonation of the hydride ligand (Equation 2). Proton affinities (PA) -ΔH_{298K} = 936 kJ mol^{-1} and 1027 kJ mol^{-1} were calculated for carbonyl and hydride ligands, respectively. The latter is slightly lower than PA values calculated for other transition metal hydride complexes (1074-1132 kJ mol^{-1}).[4] When CF_3COOH (PA = 1338 kJ mol^{-1}) was used as proton source the [Cp*MoH(COH)-$(PMe_3)_2]^+OCOCF_3^-$ ion pair product could not be optimized, all attempts leading back to the hydrogen bonded complex. These data are in support of the notion that the CO protonation pathway is not feasible. The formation enthalpy ΔH for $[Cp^*Mo(\eta^2\text{-}H_2)(CO)(PMe_3)_2]^+OCOCF_3^-$ ion pair is –328 kJ mol^{-1} relative to the isolated ions in the gas phase, which is higher than the PA difference for these ions (ΔPA = 311 kJ mol^{-1}).

The energy profiles for proton transfer from CF_3COOH to the hydride ligand of **1** were explored starting from the dihydrogen bonded complexes **B** and **D**, leading respectively to **B'** and **D'** as final products (Fig. 5). The structures of these products are depicted in Fig. 6.

Cooperative enhancement of the dihydrogen bond strength in complex **D** relative to **B** lowers the barrier substantially to only about 8 kJ mol^{1}. Taking solvent effects (under the CPCM approach) into account makes the proton transfer to the hydride ligand even more favorable, providing additional stabilization of the hydrogen bonded ion pair product (Fig. S1). This stabilization is more evident for higher polarity solvents such as THF or CH_2Cl_2.

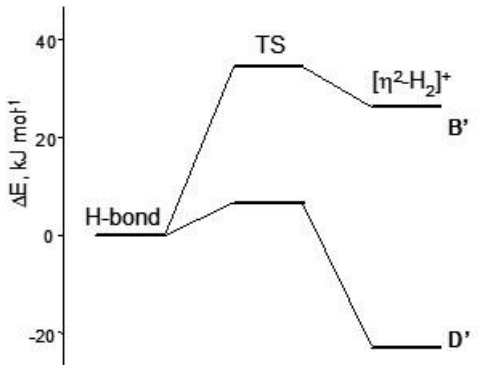

Fig. 5. Proton transfer energy profiles calculated for the reaction of **1** with one and two CF_3COOH molecules.

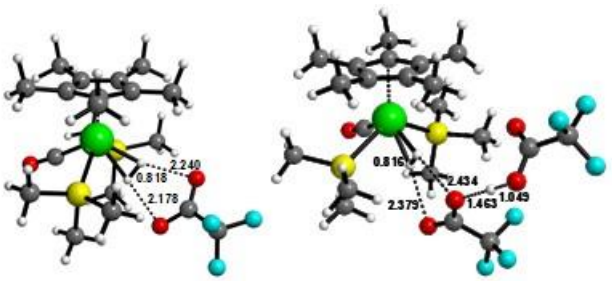

Fig. 6. Optimized structures of hydrogen bonded ion pairs as the products of proton transfer from CF_3COOH to **1**.

The occurrence of proton transfer to the hydride site was confirmed by experimental studies. Addition of 2 equiv of CF_3COOH to **1** in hexane at 200 K generates new ν_{CO} bands at1804 and 1816 cm^{-1}, assigned respectively to the dihydrogen bonded complex and $[Cp^*Mo(CO)(PMe_3)_2(\eta^2\text{-}H_2)]^+$. Corresponding bands of the hydrogen bonded acid (ν_{CO} = 1788 cm^{-1}) and of the CF_3COO anion (ν^{as}_{OCO} = 1660 cm^{-1}) are also observed. Use of excess acid makes the IR spectra uninformative. The **1**/CF_3COOD interaction was also studied by ^{1}H NMR in THF-d_8. The acid activity is reduced in THF, thus a stronger excess of the acid is necessary to promote proton transfer. A wide ^{1}H resonance at δ -4.5, assigned to the (η^2-HD) complex, appeared only in the presence of 10 equiv of acid at 200 K (Fig. S2), accompanied by $Cp^*Mo(PMe_3)_2(CO)D$ (**1**-*d*) formation by H/D exchange. Corresponding ^{31}P triplet appears at δ 32.35 and shifts to δ 32.28 with the increase of the acid amount (Fig. S2) due to the CO···HO bond formation (^{31}P resonance of **1** shifts from δ 32.0 to 31.9).

Experimental evidence for the formation of the dihydrogen bonded complex could only be obtained by IR spectroscopy on concentrated toluene solutions of **1** (of the order of 10^{-2} M instead of 10^{-3} M) in the presence of PFTB, as evidenced by a high frequency shoulder on the ν_{CO} band ($\Delta\nu_{CO}$ = 18 cm^{-1} at 250 K, Fig. S3). This complex contains most probably two alcohol molecules. The NMR monitoring in toluene-d_8 at 200 K (Fig. S4) shows, in addition to a downfield shifted hydride resonance, the presence of a broad peak at δ -4.10 with T_1 = 20

ms, characteristic for a dihydrogen complex.

The dihydrogen complex is unstable and looses H_2 upon warming, as already observed in the case of BF_4^- anion.[6] NMR monitoring of the room temperature reaction between **1** and 5 equiv of PFTB in benzene shows slow dihydrogen evolution with 46% and 68% conversion after 4 h 20 min and 49 h 40 min, respectively. At the same time the broad resonance of the alcohol proton shifts to lower fields indicating further involvment of the alcohol into hydrogen bonding. The ^{31}P NMR spectrum of this solution features peaks of different products, one of which was crystallized and analyzed by single crystal X-ray diffraction (Fig. 7).

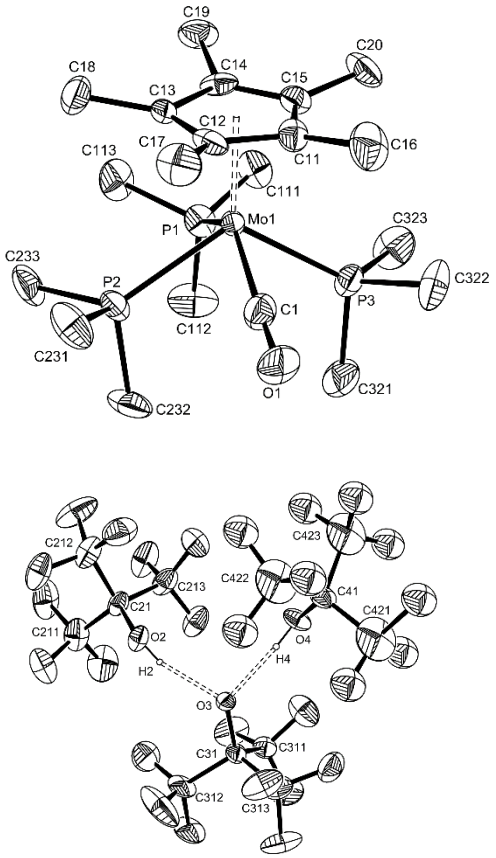

Fig. 7. Molecular structure of $[Cp^*Mo(PMe_3)_3(CO)]^+[(CF_3)_3CO{\cdot}2HOC(CF_3)_3]^-$. For the sake of clarity, the cation and the anion are shown separately. Molecular ellipsoids are shown at the 30% probability level.

The $[Cp^*Mo(PMe_3)_3(CO)]^+$ cation results from a phosphine transfer reaction. This process is closely related to the CO transfer process following the protonation of $CpMo(CO)_2(PMe_3)H$ with HBF_4, ultimately leading to $[CpMo(CO)_3(PMe_3)]^+$ through the labile $[CpMo(CO)_2(PMe_3)(H_2)]^+$.[16] It is also related to the reaction between $FeH_2(HPPh_2)_4$ and $Ph_3C^+BF_4^-$, yielding $[FeH(HPPh_2)_5]^+$ through the initial formation of the 16-electron $[FeH(HPPh_2)_4]^+$ intermediate.[17] We have shown recently that the primary product of H_2 loss from $[Cp^*Mo(\eta^2\text{-}H_2)(CO)(PMe_3)_2]^+[BF_4]^-$ - $Cp^*Mo(PMe_3)_2(CO)FBF_3$ - is not stable at ambient temperatures and slowly decomposes.[6] One of the products was identified as $Cp^*Mo(PMe_3)_2(CO)FH\cdots FBF_3$, whose formation could be rationalized taking into account the reaction between the 16-electron molybdenum fragment $[Cp^*Mo(CO)(PMe_3)_2]^+$ and F^- (generated from BF_4^-).

The interaction of **1** with the Lewis acids $Hg(C_6F_5)_2$ and $Et_2O{\cdot}BF_3$ was also briefly investigated. The interaction with $Hg(C_6F_5)_2$ (ca. 5 equiv) in *n*-hexane generated a new low frequency ν_{CO} band in the IR spectrum at 1736 cm^{-1}, demonstrating the establishment of an interaction with the carbonyl group. The relative amount of this complex (band intensity) increases upon cooling. Note that the new band is quite symmetric (Fig. 8), without any sign of a second adduct in agreement with the inability of $Hg(C_6F_5)_2$ to form complexes of higher stoichiometry.

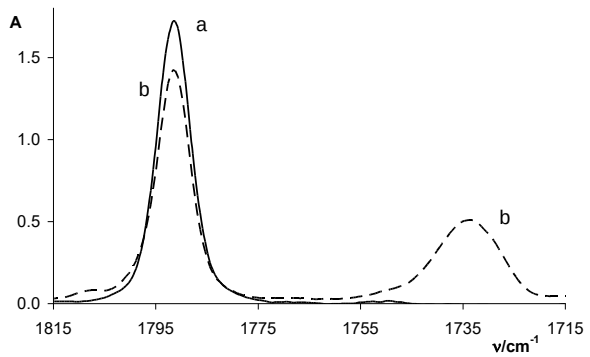

Fig. 8. IR spectra (ν_{CO} region) of $Cp^*Mo(PMe_3)_2(CO)H$ (**1**) (0.004 M) (a), **1** in the presence of ca. 5 equiv of $Hg(C_6F_5)_2$ (b). Hexane, 200 K, l = 0.12 cm

Use of $Et_2O{\cdot}BF_3$ in toluene-d_8 or THF-d_8 gives an immediate reaction at room temperature with the color changing from orange to violet. The NMR and IR data suggest formation of $[Cp^*Mo(PMe_3)_2(CO)BF_4]$.[6] In this case BF_3 presumably reacts with the hydride ligand giving initially the BHF_3^- anion, which however exchanges readily with the $Et_2O{\cdot}BF_3$ excess yielding BF_4^-. A similar observation was reported for $Cp_2Nb(CO)H$[18] and for the reaction of Cp_2TiBH_4 with $Et_2O{\cdot}BF_3$ to give $Cp_2Ti(\eta^2\text{-}BF_4)$.[19] Thus, the reactivity pattern for Lewis acids is the same as for Brønsted ones: weak acids coordinate to the CO ligand whereas strong ones interact with the hydride and ultimately lead to hydride abstraction.

Discussion

The hydrogen bonding and proton transfer equilibria described above for the $Cp^*MoH(CO)(PMe_3)_2$/ROH system can be summarized as shown in the Scheme 2, illustrating the variety of complexes formed along the reaction pathway.[10] Interaction with the carbonyl ligand oxygen atom dominates in the case of weak and medium-strength Brønsted acids (MFE, TFE, HFIP). Dihydrogen bonding (H···HOR) appears to be energetically slightly less favorable, but can be revealed in the presence of stronger acids (PFTB, CF_3COOH) at high hydride concentration. Such relation between hydrogen bonds of the two types is rather rare for transition metal carbonyl hydrido complexes; preference for CO···HOR bonding has been previously found only for $Cp^*Re(CO)_2(H)_2$.[12]

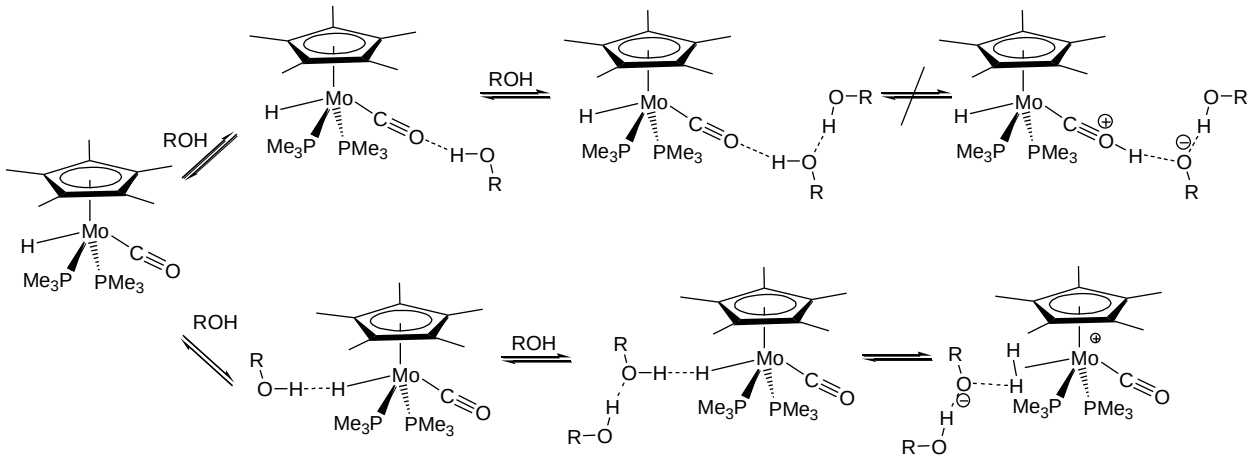

Scheme 2.

The CO···HOR interaction for group VI-VII hydride-free transition metal carbonyl complexes such as $Cp^*M(CO)_2(N_2)$ (M = Mn, Re),[12] $(C_5Et_5)M(CO)_3$ (M = Mn, Re), $(\eta^6\text{-}C_6H_3Me_3)M(CO)_3$ (M = Cr, Mo),[20] and the related NO···HOR interaction has been documented for $CpMo(CO)_2(NO)$.[20] Both interactions have been proposed to be the first step in the proton transfer to the metal atom.[20] The data described in this contribution, together with those obtained for other transition metal hydride complexes, $CpReH(CO)(NO)$,[21] $ReH_2(CO)(NO)(PR_3)_2$,[22] and $CpRuH(CO)(PCy_3)$,[5,23] show that CO···HOR or NO···HOR bonding is a "dead-end pathway", not leading to the proton transfer. In contrast, the H···HOR bond formation is the actual first reaction step. Assisted by the binding of the second proton donor molecule, which increases the hydrogen bond strength and lowers the proton transfer barrier, it leads to the $(\eta^2\text{-}H_2)$ complex formation. The results acquired up to date for molybdenum hydride complexes $Cp^*MoH(CO)(PMe_3)_2$, $Cp^*MoH(PMe_3)_3$[24] and $Cp^*MoH_3(dppe)$[15] allow explaining the different stability of $(\eta^2\text{-}H_2)$ complexes and reactivity pattern depending on the ligands (Fig. 9).

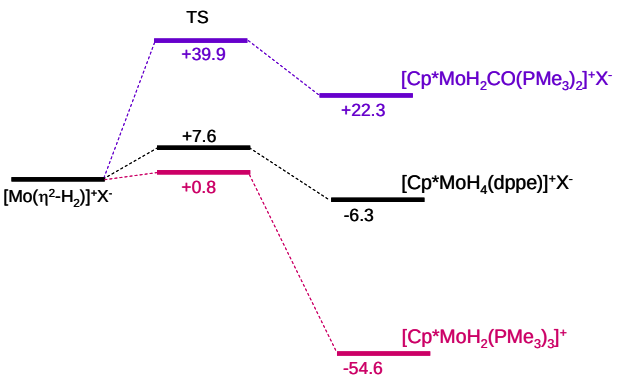

Fig. 9. Potential energy curves (ΔE, in kJ mol^{-1}) for the non-classical to classical transformations calculated at the B3LYP level in the gas phase for $[Cp^*MoH_2(PMe_3)_3]^+$,[24] $[Cp^*MoH_4(dppe)]^+[((CF_3)_2CHO)_2H]^-$,[14] and $[Cp^*MoH_2(CO)(PMe_3)_2]^+BF_4^-$.[6]

In agreement with the established mechanism of proton transfer to transition metal hydrides[9] the protonation proceeds via dihydrogen bond formation in all three cases. For the most electron reach $Cp^*MoH(PMe_3)_3$ the minimum of $(\eta^2\text{-}H_2)$ is very shallow with negligible (of 0.8 kJ mol^{-1}) barrier for isomerization to classical dihydride.[24] The latter is stabilised by 54.6 kJ mol^{-1} and thus can not convert back to the non-classical isomer in order to evolve H_2. The classical - non-classical interconversion is very easy in the case of protonated $Cp^*MoH_3(dppe)$.[15] Corresponding minima are very close in energy (-18.5 kJ mol^{-1} for the isolated cations and -6.3 kJ mol^{-1} for the $[Cp^*MoH_4(dppe)]^+[((CF_3)_2CHO)_2H]^-$ ion pair) and separated by a very low barrier (Fig. 9). Therefore, the non-classical $[Cp^*Mo(\eta^2\text{-}H_2)H_2(dppe)]^+$ intermediate could not be observed experimentally, but the classical tetrahydride complex is not thermally stable and loses dihydrogen quite easily. The $[Cp^*Mo(H)_4(dppe)]^+$ stability could be controlled by temperature and by the strength of the cation-anion interaction within the ion pair.[25] The $[Cp^*Mo(\eta^2\text{-}H_2)(CO)(PMe_3)_2]^+$/$[Cp^*Mo(H)_2(CO)(PMe_3)_2]^+$ pair of isomers is separated by a much higher barrier, whereas the relative depth of the two minima is strongly affected by the environment.[6] As the result, both could be observed experimentally but the interconversion is possible and both isomers evolve H_2 when the barrier for the latter reaction could be overcome (above 230 K).

Experimental

All manipulations were performed under an argon atmosphere. All solvents were dried over appropriate drying agent (Na/benzophenone for toluene and THF; CaH_2 for dichloromethane and hexane) and freshly distilled under an argon atmosphere prior to use. Benzene-d_6 (Euriso-Top) was kept over molecular sieves and deoxygenated with an argon flow before use. CD_2Cl_2, THF-d_8, and toluene-d_8 (Euriso-Top) were degassed by three freeze-pump-thaw cycles. Compound

$Cp^*Mo(PMe_3)_2(CO)H$ was synthesized according to the literature.[8] Et_2OHBF_4 (56%) was purchased from Sigma Aldrich and used as received. Et_2OBF_3 (48%) was purchased from Acros Organics and distilled before use.

Room temperature NMR investigations were carried out on Bruker DPX300 and Bruker AV300LiQ spectrometers operating at 300.1 MHz (^1H), 121.49 MHz ($^{31}P\{^1H\}$) and 75.47 MHz ($^{13}C\{^1H\}$). Low-temperature ^1H, $^{31}P\{^1H\}$ and $^{13}C\{^1H\}$ data were collected with Bruker AV500 spectrometer, operating at 500.3, 202.5 and 125.8 MHz, respectively. The temperature was calibrated using a methanol chemical shift thermometer; the accuracy and stability was ±1 K. All samples were allowed to equilibrate at every temperature for at least 3 min. The spectra were calibrated with the residual solvent resonance relative to TMS (^1H, ^{13}C), and with external 85% H_3PO_4 (^{31}P). The IR spectra were recorded on Specord M-82 and FT Infralum-801 spectrometers in CaF_2 cells using home modified cryostat Carl Zeiss Jena for variable temperature measurements. The accuracy of the temperature adjustment was ±1 K.

X-ray Structure Determination

Crystals of $[Cp^*Mo(PMe_3)_3(CO)]^+$ $[(CF_3)_3CO{\cdot}2HOC(CF_3)_3]^-$ complex (ν_{CO} = 1836 cm^{-1} (neat)) were grown by diffusion of pentane vapor to the mixture of **1** with 5 equiv. of PFTB in benzene. A single crystal was mounted under inert perfluoropolyether at the tip of glass fibre and cooled in the cryostream of the Oxford-Diffraction XCALIBUR CCD diffractometer. Data were collected using the monochromatic MoKα radiation (λ= 0.71073).

The structure was solved by direct methods (SIR97[26]) and refined by least-squares procedures on F^2 using SHELXL-97.[27] All H atoms attached to carbon were introduced in calculation in idealised positions and treated as riding models. The C and F atoms of one of the $(CF_3)_3COH$ anions are disordered over two positions. This disorder was modelized and treated using the tools (PART, SASI, EADP) available in SHELXL-97.[27] The drawing of the molecules was realised with the help of ORTEP32.[28] Crystal data and refinement parameters are shown in Table 4.

Crystallographic data (excluding structure factors) have been deposited with the Cambridge Crystallographic Data Centre as supplementary publication no. CCDC 742724. Copies of the data can be obtained free of charge on application to the Director, CCDC, 12 Union Road, Cambridge CB2 1EZ, UK (fax: (+44) 1223-336-033; e-mail: deposit@ccdc.cam.ac.uk).

Computational details

All calculations were performed at the DFT level, by means of the hybrid B3LYP functional,[29] as implemented in Gaussian03.[30] The LanL2DZ basis set for the Mo and P atoms was that associated with the pseudopotential[31,32] with a standard double-ζ LANL2DZ contraction,[30] supplemented in the case of P with a set of d-polarization functions.[33] The 6-31G(d) basis set was used for C atoms of Cp* ring. The 6-31++G(d,p) basis set was used for the CO group, the hydride ligand, the O and the acidic H atoms of proton donors. The 6-31G basis set was used for all other atoms. The basis set superposition error (BSSE) corrections to the gas phase complexation energies were introduced according to the counterpoise method of Boys and Bernardi.[34]

Table 4. Crystal data for $[Cp^*Mo(PMe_3)_3(CO)]^+$ $[(CF_3)_3CO{\cdot}2HOC(CF_3)_3]^-$

Empirical formula	$C_{20}H_{42}MoOP_3$, $C_{12}H_2F_{27}O_3$
Formula weight	1194.52
Color	orange
Temperature, K	180(2)
Wavelength, Å	0.71073
Crystal system	Orthorhombic
Space group	P b c a
a, Å	16.2134(4)
b, Å	20.3539(6)
c, Å	27.5461(7)
α, °	90.0
β, °	90.0
γ, °	90.0
Volume, $Å^3$	9090.4(4)
Z	8
Density (calculated), Mg/m^3	1.746
Absorption coefficient, mm^{-1}	0.541
F(000)	4784
Crystal size, mm^3	0.48 x 0.24 x 0.10 mm^3
Theta range, °	2.70 to 26.37
Reflections collected	66640
Independent reflections (R_{int})	9284 (0.100)
Completeness, %	99.8
Absorption correction	Multi-scan
Max. and min. transmission	1.000 and 0.558
Refinement method	F^2
Data / restraints / parameters	9284 / 120 / 602
Goodness-of-fit on F^2	1.099
R1, wR2 [I>2σ(I)]	0.0858, 0.1871
R1, wR2 (all data)	0.1917, 0.2715
Residual density, $e.Å^{-3}$	1.840 / -0.923 e.Å

Additional calculations of H-complexes between **1** and CH_3OH and of free reactants were performed using pseudopotential-based correlation consistent polarized valence triple-ζ basis set cc-pVTZ-PP[35] for Mo and 6-31G(d) basis set for P atoms. The differently optimized structures of **1** with the two above described basis sets do not differ by more than 0.020 Å for Mo-C bond distances and 0.008 Å for Mo-P, Mo-H and C-O bond distances. The formation energy of adduct **A** (see Table 3 for the legend) increases by only 1 kJ mol^{-1} while that of adduct **B** remains the same as do their geometries. The frequency shifts (Δν) resulting from hydrogen bond formation differ by no more than 2%, except for $\Delta\nu_{OH}$ of complex **A** which increases by 5%.

The structures of the reactants, intermediates, transition states, and products were fully optimized without any symmetry restriction. Transition states were identified by having one imaginary frequency in the Hessian matrix. No scaling factor was applied to the calculated frequencies since the optimization was run in the gas phase and the IR spectra were measured in solution.

Non-specific solvent effects were introduced through CPCM continuum representation of the solvent by single-point calculations[36] on gas phase optimized geometries for toluene (ε = 2.38), dichloromethane (ε = 8.93) and THF (ε = 7.58). The

G^{solv} values account for the solvation free energies, with inclusion of the solute free energy contributions $\Delta G^{solv} = \Delta E^{solv} + \Delta G^{gas} - \Delta E^{gas}$, where ΔE^{solv} is the electronic energy plus the solvent entropy.[37] The optimisations of **1**, CF_3COOH and their dihydrogen bonded adduct **B** were also performed in THF, leading to only minor geometry changes for **1** and CF_3COOH ($\Delta r < 0.01$ Å), while the H···H bond length in **B** increased by 0.026 Å. Despite this lengthening, the interaction energy decreased by only 0.3 (ΔE^{solv}) and 0.1 kJ mol^{-1} (ΔG^{solv}). The same pattern was revealed for stronger dihydrogen bonded complexes of anionic main group tetrahydrides optimisations in solution.[38] Therefore the consideration of solvent effects was kept within the single point CPCM approach for the rest of the study.

Conclusions

We presented results of combined spectroscopic and theoretical investigations of hydrogen bonding to $Cp^*MoH(CO)(PMe_3)_2$ and its role in the proton transfer process. The formation of several hydrogen bonded complexes involving both carbonyl and hydride ligands was observed experimentally; their structures and spectroscopic features were also studied by DFT calculations. The CO···HOR type of bonding was found to dominate over the MoH···HOR one, which is a rather rare occurrence. However, only the MoH···HOR adduct is the intermediate of the proton transfer reaction yielding the non-classical cation $[Cp^*Mo(\eta^2\text{-}H_2)(CO)(PMe_3)_2]^+$.

Acknowledgment

Support of this work through France-Russia bilateral programs (PICS grant 2004-07, continuing within the framework of a GDRE (groupe de recherche européen) 2008-11 (RFBR-CNRS grant 08-03-92506)) and support of the RFBR (08-03-00464) is gratefully acknowledged. Additional national support was obtained in France from the CNRS, the IUF, and in Russia from the Division of Chemistry and Material Sciences of RAS and the Russian Federation President grant (MK-380.2008.3). RP thanks the CICT for granting free computational time.

Captions for figures

Fig. 6. Hydride region of the ^1H NMR (500.3 MHz) spectrum of $Cp^*Mo(PMe_3)_2(CO)H$ (**1**) alone (a), and in the presence of 2 equiv. (b) or 4.5 equiv. (c) of TFE. T = 200K, CD_2Cl_2, c(**1**) = $5.8 \cdot 10^{-2}$ M.

Fig. 7. $^{13}C\{^1H\}$ NMR (125.8MHz, CO region) spectrum of $Cp^*Mo(PMe_3)_2(CO)H$ (**1**) (a) and **1** in the presence of ca. 2 equiv. PFTB (b). Toluene-d_8, 200K. c(**1**) = $1 \cdot 10^{-1}$ M, 1330 scans.

Fig. 8. IR spectra (ν_{CO} region) of $Cp^*Mo(PMe_3)_2(CO)H$ (**1**) (0.005 M) (a) and in the presence of ca. 3 equiv. TFE (b), 3 equiv HFIP (c), 3 equiv PFTB (d). T = 200K, hexane, l = 1.2 mm.

Fig. 9. Optimized geometries of hydrogen bonded complexes between **1** and one and two CH_3OH molecules.

Fig. 10. Proton transfer energy profiles calculated for the reaction of **1** with one and two CF_3COOH molecules.

Fig. 6. Optimized structures of hydrogen bonded ion pairs as the products of proton transfer from CF_3COOH to **1**.

Fig. 7. Molecular structure of $[Cp^*Mo(PMe_3)_3(CO)]^+[(CF_3)_3CO{\cdot}2HO\text{-}C(CF_3)_3]^-$. For the sake of clarity, the cation and the anion are shown separately. Molecular ellipsoids are shown at the 30% probability level.

Fig. 8. IR spectra (ν_{CO} region) of $Cp^*Mo(PMe_3)_2(CO)H$ (**1**) (0.004 M) (a), **1** in the presence of 5 equiv of $Hg(C_6F_5)_2$ (b). Hexane, 200 K, l = 0.12 cm

Fig. 9. Potential energy curves (ΔE, in kJ mol^{-1}) for the non-classical to classical transformations calculated at the B3LYP level in the gas phase for $[Cp^*MoH_2(PMe_3)_3]^+$,[24] $[Cp^*MoH_4(dppe)]^+[((CF_3)_2CHO)_2H]^-$,[14] and $[Cp^*MoH_2(CO)(PMe_3)_2]^+BF_4^-$.[6]

Notes and references

[a] *A. N. Nesmeyanov Institute of Organoelement Compounds, Russian Academy of Sciences, Vavilov Street 28, 119991 Moscow, Russia Fax: +7 499 1355085; Tel: +7 499 1356448; E-mail: nataliabelk@ineos.ac.ru*
[b] *CNRS; LCC (Laboratoire de Chimie de Coordination); Université de Toulouse; UPS, INPT; 205, route de Narbonne, F-31077 Toulouse, France*
[c] *Institut Universitaire de France, 103, bd Saint-Michel, 75005 Paris, France*

† Electronic Supplementary Information (ESI) available: selected NMR and IR data; geometrical parameters for the hydrogen-bonded complexes calculated; XYZ tables for all the molecules calculated; crystallographic data in CIF format. See DOI: 10.1039/b000000x/

1 C. Elschenbroich, A. Salzer, *Organometallics: A Concise Introduction*, VCH, New York, 2nd edn., 1992
2 C. P. Horwit and D. F. Shriver, *Adv. Organomet. Chem.* 1984, **23**, 219 and references therein
3 S. S. Kristjánsdóttir and J. R. Norton, in *Transition Metal Hydrides*, ed. A. Dedieu, VCH, New York, 1992, pp 309; K. H. Whitmire and D. F. Shriver, *J. Am. Chem. Soc.* 1981, **103**, 6755-6757; L. R. Nevinger, J. B. Keister and J. Maher, *Organometallics* 1990, **9**, 1900-1905; D. C. Pribich and E. Rosenberg, *Organometallics* 1988, **7**, 1741-1745.
4 N. V. Belkova, L. M. Epstein and E. S. Shubina, *ARKIVOC*, 2008 (iv), 120-138.
5 N.V. Belkova, M. Besora, L.M. Epstein, A. Lledós, F. Maseras and E.S. Shubina, *J. Am. Chem. Soc.* 2003, **125**, 7715-7725
6 P. A. Dub, N. V. Belkova, O. A. Filippov, J.-C. Daran, L. M. Epstein, A. Lledós, E. S. Shubina and R. Poli, *Chem. Eur. J.* 2009, DOI: 10.1002/chem.200901613.
7 M.-J. Tudoret, M.-L. Robo and C. Lapinte, *Organometallics* 1992, **11**, 1419–1422
8 J. H. Shin, D. G. Churchill and G. Parkin, *J. Organomet. Chem.* 2002, **642**, 9-15
9 N. V. Belkova, E. S. Shubina and L.M. Epstein. *Acc. Chem. Res.* 2005, **38**, 624-631.
10 M. Besora, A. Lledós and F. Maseras *Chem. Soc. Rev.*, 2009, **38**, 957–966
11 L.M. Epstein, N.V. Belkova, E.I. Gutsul and E.S. Shubina, *Polish J. Chem.*, 2003, **77**, 1371-1383.
12 P. A. Hamley, S. G. Kazarian and M. Poliakoff, *Organometallics* 1994, **13**, 1767-1774.
13 A. V. Iogansen, *Theor. Exp. Chem.* 1971, **7**, 312–317; A. V. Iogansen, *Spectrochim. Acta, Part A* 1999, **55**, 1585–1612.
14 N. V. Belkova, P. O. Revin, M. Besora, M. Baya, L. M. Epstein, A. Lledós, R. Poli, E. S. Shubina and E. V. Vorontsov, *Eur. J.Inorg. Chem.*, 2006, 2192-2209
15 T. Steiner *Angew. Chem. Int. Ed.*, 2002, **41**, 48-76
16 E. A. Quadrelli, H.-B. Kraatz and R. Poli, *Inorg. Chem.* 1996, **35**, 5154-5162.
17 J. R. Sanders, *J. Chem. Soc. Dalton Trans.* 1972, 1333-1336.
18 E. E. H.Otto and H. H. Brintzinger, *J. Organomet. Chem.* 1979, **170**, 209-216.
19 H. Nöth and R. Hartwimmer, *Chem. Ber.* 1960, **93**, 2246-2251.

20 B.V. Lokshin, A.G. Ginsburg and S.G. Kazaryan, *J. Mol. Str.* 1988, **174**, 29-34
21 E. S. Shubina, N. V. Belkova, A.V. Ionidis, N.S. Golubev, S.N. Smirnov, P. Schah-Mohammedi and L.M. Epstein, *Izv. Akad. Nauk, Ser. Khim.* 1997, 1405-1407 (*Russ. Chem. Bull.* 1997, **44**, 1349-1351)
22 N.V. Belkova, E.S. Shubina, A.V. Ionidis, L.M. Epstein, H. Jacobsen, A. Messmer and H. Berke, *Inorg. Chem.*, 1997, **36**, 1522-1525; N.V. Belkova, E.S. Shubina, E.I. Gutsul, L.M. Epstein, I.L. Eremenko and S.E. Nefedov, *J. Organomet. Chem.*, 2000, **610**, 58-70.
23 N.V. Belkova, A.V. Ionidis, L.M. Epstein, E.S. Shubina, S. Gruendemann, N.S. Golubev and H.-H. Limbach, *Eur J. Inorg. Chem.*, 2001, 1753-1761.
24 M. Baya, P. A. Dub, J. Houghton, J.-C. Daran, N. V. Belkova, E. S. Shubina, L. M. Epstein, A. Lledós, and R. Poli, *Inorg. Chem.* 2009, **48**, 209-220.
25 P. A. Dub, M. Baya, J. Houghton, N. V. Belkova, J.-C. Daran, R. Poli, L. M. Epstein and E. S. Shubina, *Eur. J. Inorg. Chem.*, 2007, 2813-2826.
26 Altomare, A.; Burla, M.C.; Camalli, M.; Cascarano, G.L.; Giacovazzo, C.; Guagliardi, A.; Moliterni, A.G.G.; Polidori, G.; Spagn, R. *J. Appl. Cryst.* 1999, **32**, 115.
27 Sheldrick, G.M. *Acta Cryst.*, 2008, **A64**, 112-122.
28 Farrugia, L. J. ORTEP3 for Windows, *J. Appl. Cryst.* 1997, **30**, 565.
29 A. D. Becke, *J. Chem. Phys.* 1993, **98**, 5648-5652; C. T. Lee, W. T. Yang and R. G. Parr, *Phys. Rev. B* 1988, **37**, 785-789; P. Stephens, F. Devlin, C. Chabalowski and M. Frisch, *J. Phys. Chem.* 1994, **98**, 11623-11627.
30 M. J. Frisch, G. W. Trucks, H. B. Schlegel, G. E. Scuseria, M. A. Robb, J. R. Cheeseman, J. Montgomery, J. A., T. Vreven, K. N. Kudin, J. C. Burant, J. M. Millam, S. S. Iyengar, J. Tomasi, V. Barone, B. Mennucci, M. Cossi, G. Scalmani, N. Rega, G. A. Petersson, H. Nakatsuji, M. Hada, M. Ehara, K. Toyota, R. Fukuda, J. Hasegawa, M. Ishida, T. Nakajima, Y. Honda, O. Kitao, H. Nakai, M. Klene, X. Li, J. E. Knox, H. P. Hratchian, J. B. Cross, C. Adamo, J. Jaramillo, R. Gomperts, R. E. Stratmann, O. Yazyev, A. J. Austin, R. Cammi, C. Pomelli, J. W. Ochterski, P. Y. Ayala, K. Morokuma, G. A. Voth, P. Salvador, J. J. Dannenberg, V. G. Zakrzewski, S. Dapprich, A. D. Daniels, M. C. Strain, O. Farkas, D. K. Malick, A. D. Rabuck, K. Raghavachari, J. B. Foresman, J. V. Ortiz, Q. Cui, A. G. Baboul, S. Clifford, J. Cioslowski, B. B. Stefanov, G. Liu, A. Liashenko, P. Piskorz, I. Komaromi, R. L. Martin, D. J. Fox, T. Keith, M. A. Al-Laham, C. Y. Peng, A. Nanayakkara, M. Challacombe, P. M. W. Gill, B. Johnson, W. Chen, M. W. Wong, C. Gonzalez and J. A. Pople, Gaussian 03, Revision D.01, Gaussian, Inc., Wallingford CT, 2004
31 P. J. Hay and W. R. Wadt, *J. Chem. Phys.* 1985, **82**, 270-283.
32 W. R. Wadt and P. J. Hay, *J. Chem. Phys.* 1985, **82**, 284-298.
33 A. Höllwarth, M. Böhme, S. Dapprich, A. Ehlers, A. Gobbi, V. Jonas, K. Kohler, R. Stegmann, A. Veldkamp and G. Frenking, *Chem. Phys. Lett.* 1993, **208**, 237-40
34 S. F. Boys and F. Bernardi, *Mol. Phys.* 1970, **19**, 553-566.
35 K.A. Peterson, D. Figgen, M. Dolg, and H. Stoll, *J. Chem. Phys.* 2007, **126**, 124101.
36 V. Barone and M. Cossi, *J. Phys. Chem. A* 1998, **102**, 1995-2001; M. Cossi, N. Rega, G. Scalmani and V. Barone, *J. Comput. Chem.* 2003, **24**, 669-681.
37 A. A. C. Braga, G. Ujaque and F. Maseras, *Organometallics* 2006, **25**, 3647-3658.
38 O.A. Filippov, A.M. Filin, V.N. Tsupreva, N.V. Belkova, A. Lledos, G. Ujaque, L.M. Epstein and E.S. Shubina, *Inorg. Chem.* 2006, **45**, 3086-3096.